The QCD Phase Diagram

Rajiv V. Gavai and Sourendu Gupta
T. I. F. R., Mumbai

The QCD Phase Diagram

Rajiv V. Gavai and Sourendu Gupta
T. I. F. R., Mumbai

Introduction

Expected QCD Phase Diagram

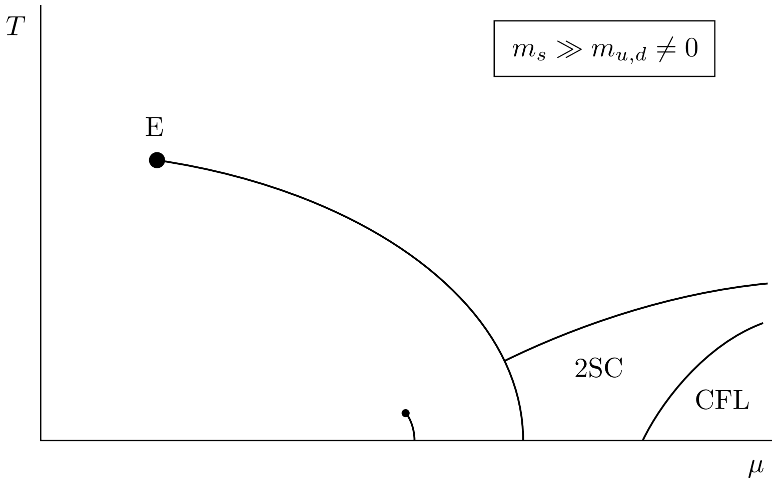

Introduction

Expected QCD Phase Diagram

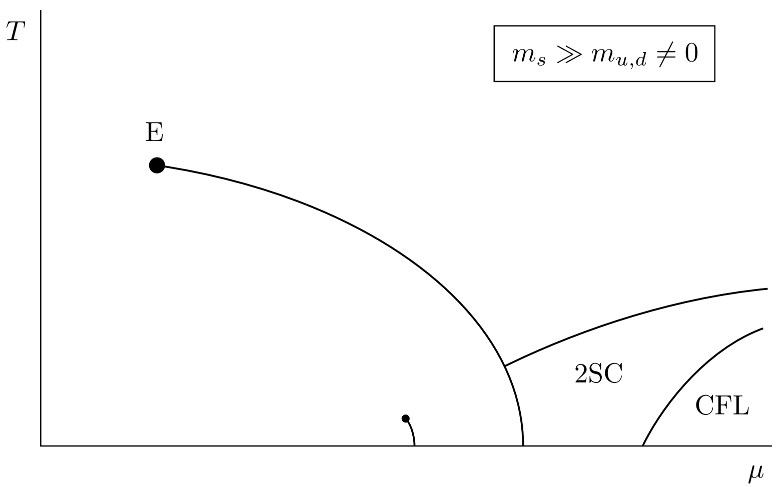

... but could, however, be ...

Introduction

Expected QCD Phase Diagram

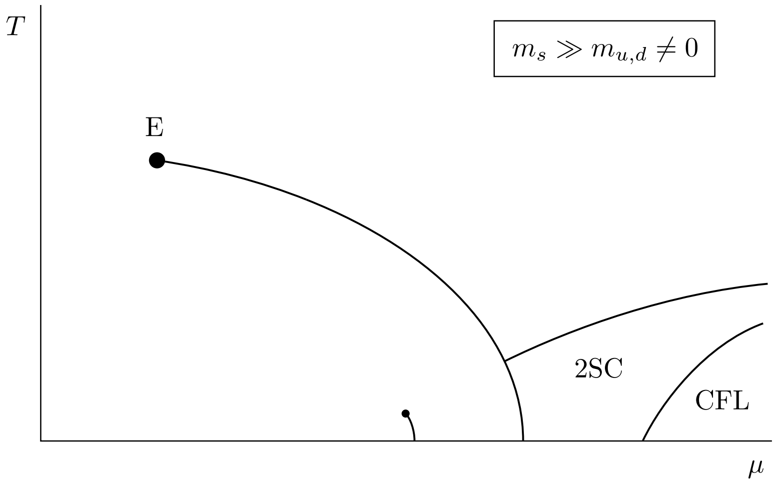

... but could, however, be ...

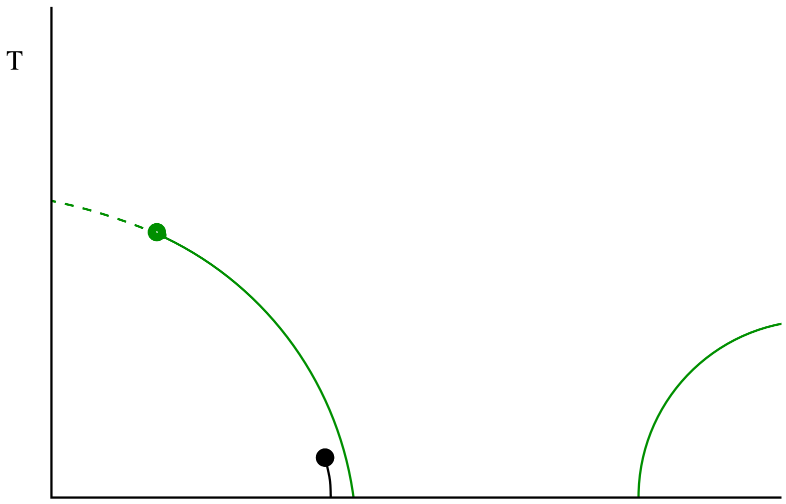

Assuming N_f flavours of quarks, and denoting by μ_f the corresponding chemical potentials, the QCD partition function is

$$\mathcal{Z} = \int DU \exp(-S_G) \ \prod_f \mathrm{Det} \ M(m_f, \mu_f) \quad .$$

Assuming N_f flavours of quarks, and denoting by μ_f the corresponding chemical potentials, the QCD partition function is

$$\mathcal{Z} = \int DU \exp(-S_G) \prod_f \mathrm{Det}\ M(m_f, \mu_f) \quad .$$

Since $\gamma_5 M^\dagger(\mu)\gamma_5 = M(-\mu)$, $\mathrm{Det}^*\ M(\mu) = \mathrm{Det}\ M(-\mu) \neq \mathrm{Det}\ M(\mu)$, i.e., Det M is complex, $\Longrightarrow$ Phase (Sign) problem !

Assuming N_f flavours of quarks, and denoting by μ_f the corresponding chemical potentials, the QCD partition function is

$$\mathcal{Z} = \int DU \exp(-S_G) \ \prod_f \mathrm{Det} \ M(m_f, \mu_f) \quad .$$

Since $\gamma_5 M^\dagger(\mu)\gamma_5 = M(-\mu)$, $\mathrm{Det}^* \ M(\mu) = \mathrm{Det} \ M(-\mu) \neq \mathrm{Det} \ M(\mu)$, i.e., Det M is complex, $\Longrightarrow$ Phase (Sign) problem !

Lattice Approaches to unravel the Phase Diagram:

- Lee-Yang zeroes and Two parameter Re-weighting (Z. Fodor & S. Katz, JHEP 0203 (2002) 014).

Assuming N_f flavours of quarks, and denoting by μ_f the corresponding chemical potentials, the QCD partition function is

$$\mathcal{Z} = \int DU \exp(-S_G) \prod_f \mathrm{Det}\ M(m_f, \mu_f) \quad .$$

Since $\gamma_5 M^\dagger(\mu)\gamma_5 = M(-\mu)$, $\mathrm{Det}^*\ M(\mu) = \mathrm{Det}\ M(-\mu) \neq \mathrm{Det}\ M(\mu)$, i.e., Det M is complex, $\Longrightarrow$ Phase (Sign) problem !

Lattice Approaches to unravel the Phase Diagram:

- Lee-Yang zeroes and Two parameter Re-weighting (Z. Fodor & S. Katz, JHEP 0203 (2002) 014).
- Imaginary Chemical Potential (Ph. de Forcrand & O. Philipsen, NP B642 (2002) 290; M.-P. Lombardo & M. D'Elia PR D67 (2003) 014505).

Assuming N_f flavours of quarks, and denoting by μ_f the corresponding chemical potentials, the QCD partition function is

$$\mathcal{Z} = \int DU \exp(-S_G) \prod_f \mathrm{Det}\ M(m_f, \mu_f) \quad .$$

Since $\gamma_5 M^\dagger(\mu)\gamma_5 = M(-\mu)$, $\mathrm{Det}^*\ M(\mu) = \mathrm{Det}\ M(-\mu) \neq \mathrm{Det}\ M(\mu)$,
i.e., Det M is complex, $\Longrightarrow$ Phase (Sign) problem !

Lattice Approaches to unravel the Phase Diagram:

- Lee-Yang zeroes and Two parameter Re-weighting (Z. Fodor & S. Katz, JHEP 0203 (2002) 014).
- Imaginary Chemical Potential (Ph. de Forcrand & O. Philipsen, NP B642 (2002) 290; M.-P. Lombardo & M. D'Elia PR D67 (2003) 014505).
- Taylor Expansion (C. Allton et al., PR D66 (2002) 074507 & D68 (2003) 014507; R.V. Gavai and S. Gupta, PR D68 (2003) 034506).

Why Taylor series expansion?

- Ease of taking continuum and thermodynamic limit

Why Taylor series expansion?

- Ease of taking continuum and thermodynamic limit

- E.g., $\exp[\Delta S]$ factor makes this exponentially tough for re-weighting.

Why Taylor series expansion?

- Ease of taking continuum and thermodynamic limit

- E.g., $\exp[\Delta S]$ factor makes this exponentially tough for re-weighting.

- Discretization errors propagate in an unknown manner in re-weighting.

Why Taylor series expansion?

- Ease of taking continuum and thermodynamic limit
- E.g., exp$[\Delta S]$ factor makes this exponentially tough for re-weighting.
- Discretization errors propagate in an unknown manner in re-weighting.
- Reweighting reasonable for only small μ ? (Ejiri 2004)

Why Taylor series expansion?

- Ease of taking continuum and thermodynamic limit
- E.g., $\exp[\Delta S]$ factor makes this exponentially tough for re-weighting.
- Discretization errors propagate in an unknown manner in re-weighting.
- Reweighting reasonable for only small μ ? (Ejiri 2004)

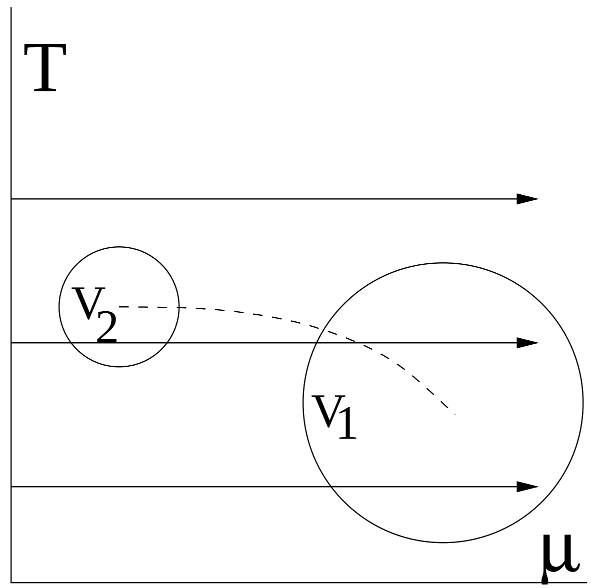

We study volume dependence at several T to i) bracket the critical region and then to ii) track its change as a function of volume.

Methodology

From the QCD partition function

$$\mathcal{Z} = \int DU \exp(-S_G) \ \prod_f \mathrm{Det} \ M(m_f, \mu_f) \quad ,$$

various number densities and susceptibilities are obtained using canonical definitions :

$$n_i = \frac{T}{V}\frac{\partial \ln \mathcal{Z}}{\partial \mu_i} \text{ and } \qquad \chi_{ij} = \frac{T}{V}\frac{\partial^2 \ln \mathcal{Z}}{\partial \mu_i \partial \mu_j} \quad .$$

Higher order susceptibilities are defined by

$$\chi_{fg\cdots} = \frac{T}{V}\frac{\partial^n \log Z}{\partial \mu_f \partial \mu_g \cdots} = \frac{\partial^n P}{\partial \mu_f \partial \mu_g \cdots} \ . \tag{1}$$

Methodology

From the QCD partition function

$$\mathcal{Z} = \int DU \exp(-S_G) \prod_f \mathrm{Det}\ M(m_f, \mu_f) \quad ,$$

various number densities and susceptibilities are obtained using canonical definitions :

$$n_i = \frac{T}{V}\frac{\partial \ln \mathcal{Z}}{\partial \mu_i} \text{ and } \qquad \chi_{ij} = \frac{T}{V}\frac{\partial^2 \ln \mathcal{Z}}{\partial \mu_i \partial \mu_j} \quad .$$

Higher order susceptibilities are defined by

$$\chi_{fg\cdots} = \frac{T}{V}\frac{\partial^n \log Z}{\partial \mu_f \partial \mu_g \cdots} = \frac{\partial^n P}{\partial \mu_f \partial \mu_g \cdots} \ . \tag{1}$$

Methodology

From the QCD partition function

$$\mathcal{Z} = \int DU \exp(-S_G) \prod_f \mathrm{Det} \; M(m_f, \mu_f) \quad ,$$

various number densities and susceptibilities are obtained using canonical definitions :

$$n_i = \frac{T}{V}\frac{\partial \ln \mathcal{Z}}{\partial \mu_i} \text{ and } \qquad \chi_{ij} = \frac{T}{V}\frac{\partial^2 \ln \mathcal{Z}}{\partial \mu_i \partial \mu_j} \quad .$$

Higher order susceptibilities are defined by

$$\chi_{fg\cdots} = \frac{T}{V}\frac{\partial^n \log Z}{\partial \mu_f \partial \mu_g \cdots} = \frac{\partial^n P}{\partial \mu_f \partial \mu_g \cdots} \, . \tag{1}$$

These are Taylor coefficients of the pressure P in its expansion in μ.

$$\frac{\Delta P}{T^4} \equiv \frac{P(\mu,T)}{T^4} - \frac{P(0,T)}{T^4} = \sum_{n_u,n_d} \chi_{n_u,n_d} \frac{1}{n_u!} \left(\frac{\mu_u}{T}\right)^{n_u} \frac{1}{n_d!} \left(\frac{\mu_d}{T}\right)^{n_d} \qquad (2)$$

From this a series for baryonic susceptibility can be constructed. Its radius of convergence gives the nearest critical point.

For 2 light flavours, its coefficients up to 6th order in $\mu_B/3 = \mu_u = \mu_d$ are

$$\chi_B^0 = \chi_{20}, \qquad \chi_B^4 = \frac{1}{4!}\left[\chi_{60} + 4\chi_{51} + 7\chi_{42} + 4\chi_{33}\right],$$

$$\chi_B^2 = \frac{1}{2!}\left[\chi_{40} + 2\chi_{31} + \chi_{22}\right], \qquad \chi_B^6 = \frac{1}{6!}\left[\chi_{80} + 6\chi_{71} + 16\chi_{62} + 26\chi_{53} + 15\chi_{44}\right]. \qquad (3)$$

These are Taylor coefficients of the pressure P in its expansion in μ.

$$\frac{\Delta P}{T^4} \equiv \frac{P(\mu,T)}{T^4} - \frac{P(0,T)}{T^4} = \sum_{n_u,n_d} \chi_{n_u,n_d} \frac{1}{n_u!} \left(\frac{\mu_u}{T}\right)^{n_u} \frac{1}{n_d!} \left(\frac{\mu_d}{T}\right)^{n_d} \tag{2}$$

From this a series for baryonic susceptibility can be constructed. Its radius of convergence gives the nearest critical point.

For 2 light flavours, its coefficients up to 6th order in $\mu_B/3 = \mu_u = \mu_d$ are

$$\begin{aligned} \chi_B^0 &= \chi_{20}, & \chi_B^4 &= \frac{1}{4!}\left[\chi_{60} + 4\chi_{51} + 7\chi_{42} + 4\chi_{33}\right], \\ \chi_B^2 &= \frac{1}{2!}\left[\chi_{40} + 2\chi_{31} + \chi_{22}\right], & \chi_B^6 &= \frac{1}{6!}\left[\chi_{80} + 6\chi_{71} + 16\chi_{62} + 26\chi_{53} + 15\chi_{44}\right]. \end{aligned} \tag{3}$$

These are Taylor coefficients of the pressure P in its expansion in μ.

$$\frac{\Delta P}{T^4} \equiv \frac{P(\mu,T)}{T^4} - \frac{P(0,T)}{T^4} = \sum_{n_u,n_d} \chi_{n_u,n_d} \frac{1}{n_u!} \left(\frac{\mu_u}{T}\right)^{n_u} \frac{1}{n_d!} \left(\frac{\mu_d}{T}\right)^{n_d} \qquad (2)$$

From this a series for baryonic susceptibility can be constructed. Its radius of convergence gives the nearest critical point.

For 2 light flavours, its coefficients up to 6th order in $\mu_B/3 = \mu_u = \mu_d$ are

$$\chi_B^0 = \chi_{20}, \qquad \chi_B^4 = \frac{1}{4!}\left[\chi_{60} + 4\chi_{51} + 7\chi_{42} + 4\chi_{33}\right],$$
$$\chi_B^2 = \frac{1}{2!}\left[\chi_{40} + 2\chi_{31} + \chi_{22}\right], \qquad \chi_B^6 = \frac{1}{6!}\left[\chi_{80} + 6\chi_{71} + 16\chi_{62} + 26\chi_{53} + 15\chi_{44}\right]. \qquad (3)$$

Successive estimates for the radius of convergence can be obtained from these using

$$\rho_n = \left[\left|\frac{\chi_B^0}{\chi_B^n}\right|\right]^{\frac{1}{n}} \qquad \text{or} \qquad r_{2n+2} = \sqrt{\left|\frac{\chi_B^{2n}}{\chi_B^{2n+2}}\right|}.$$

Similar coefficients for the off-diagonal susceptibility are

$$\underline{\chi}_B^0 = \chi_{11}, \qquad \underline{\chi}_B^2 = \frac{1}{2!}\left[2\chi_{31} + 2\chi_{22}\right],$$
$$\underline{\chi}_B^4 = \frac{1}{4!}\left[2\chi_{51} + 8\chi_{42} + 6\chi_{33}\right], \qquad \underline{\chi}_B^6 = \frac{1}{6!}\left[2\chi_{71} + 12\chi_{62} + 30\chi_{53} + 20\chi_{44}\right] \tag{4}$$

♡ The ratio χ_{11}/χ_{20} can be shown to yield the ratio of widths of the measure in the imaginary and real directions at $\mu = 0$.

♡ Can be generalized to nonzero μ with some care and the coefficients above.

Successive estimates for the radius of convergence can be obtained from these using

$$\rho_n = \left[\left| \frac{\chi_B^0}{\chi_B^n} \right| \right]^{\frac{1}{n}} \qquad \text{or} \qquad r_{2n+2} = \sqrt{\left| \frac{\chi_B^{2n}}{\chi_B^{2n+2}} \right|}.$$

Similar coefficients for the off-diagonal susceptibility are

$$\underline{\chi}_B^0 = \chi_{11}, \qquad \underline{\chi}_B^2 = \frac{1}{2!}\left[2\chi_{31} + 2\chi_{22}\right],$$
$$\underline{\chi}_B^4 = \frac{1}{4!}\left[2\chi_{51} + 8\chi_{42} + 6\chi_{33}\right], \qquad \underline{\chi}_B^6 = \frac{1}{6!}\left[2\chi_{71} + 12\chi_{62} + 30\chi_{53} + 20\chi_{44}\right] \quad (4)$$

♡ The ratio χ_{11}/χ_{20} can be shown to yield the ratio of widths of the measure in the imaginary and real directions at $\mu = 0$.

♡ Can be generalized to nonzero μ with some care and the coefficients above.

Successive estimates for the radius of convergence can be obtained from these using

$$\rho_n = \left[\left|\frac{\chi_B^0}{\chi_B^n}\right|\right]^{\frac{1}{n}} \qquad \text{or} \qquad r_{2n+2} = \sqrt{\left|\frac{\chi_B^{2n}}{\chi_B^{2n+2}}\right|}.$$

Similar coefficients for the off-diagonal susceptibility are

$$\underline{\chi}_B^0 = \chi_{11}, \qquad \underline{\chi}_B^2 = \frac{1}{2!}\left[2\chi_{31} + 2\chi_{22}\right],$$
$$\underline{\chi}_B^4 = \frac{1}{4!}\left[2\chi_{51} + 8\chi_{42} + 6\chi_{33}\right], \qquad \underline{\chi}_B^6 = \frac{1}{6!}\left[2\chi_{71} + 12\chi_{62} + 30\chi_{53} + 20\chi_{44}\right] \quad (4)$$

♡ The ratio χ_{11}/χ_{20} can be shown to yield the ratio of widths of the measure in the imaginary and real directions at $\mu = 0$.

♡ Can be generalized to nonzero μ with some care and the coefficients above.

Successive estimates for the radius of convergence can be obtained from these using

$$\rho_n = \left[\left| \frac{\chi_B^0}{\chi_B^n} \right| \right]^{\frac{1}{n}} \qquad \text{or} \qquad r_{2n+2} = \sqrt{\left| \frac{\chi_B^{2n}}{\chi_B^{2n+2}} \right|}.$$

Similar coefficients for the off-diagonal susceptibility are

$$\underline{\chi}_B^0 = \chi_{11}, \qquad \underline{\chi}_B^2 = \frac{1}{2!}\left[2\chi_{31} + 2\chi_{22}\right],$$

$$\underline{\chi}_B^4 = \frac{1}{4!}\left[2\chi_{51} + 8\chi_{42} + 6\chi_{33}\right], \qquad \underline{\chi}_B^6 = \frac{1}{6!}\left[2\chi_{71} + 12\chi_{62} + 30\chi_{53} + 20\chi_{44}\right] \quad (4)$$

♡ The ratio χ_{11}/χ_{20} can be shown to yield the ratio of widths of the measure in the imaginary and real directions at $\mu = 0$.

♡ Can be generalized to nonzero μ with some care and the coefficients above.

The Susceptibilities

All susceptibilities can be written as traces of products of M^{-1} and various derivatives of M.
Two steps for getting NLS : 1) Writing down in terms of derivatives of Z and 2) obtaining these derivatives in terms of traces.

Setting $\mu_i = 0$, χ's are nontrivial for only even $N = n_u + n_d$. Thus at leading order,

$$\chi_{20} = \left(\frac{T}{V}\right)\frac{Z_{20}}{Z} \qquad \chi_{11} = \left(\frac{T}{V}\right)\frac{Z_{11}}{Z} \tag{5}$$

Here $Z_{20} = Z[\langle \mathcal{O}_2 + \mathcal{O}_{11} \rangle]$, $Z_{11} = Z[\langle \mathcal{O}_{11} \rangle]$, $\mathcal{O}_1 = \mathrm{Tr}\ M^{-1}M'$,
$\mathcal{O}_2 = \mathcal{O}_1' = \mathrm{Tr}\ M^{-1}M'' - \mathrm{Tr}\ M^{-1}M'M^{-1}M'$, and
$\mathcal{O}_{11} = \mathcal{O}_1 \cdot \mathcal{O}_1 = (\mathrm{Tr}\ M^{-1}M')^2$.

The Susceptibilities

All susceptibilities can be written as traces of products of M^{-1} and various derivatives of M.
Two steps for getting NLS : 1) Writing down in terms of derivatives of Z and 2) obtaining these derivatives in terms of traces.

Setting $\mu_i = 0$, χ's are nontrivial for only even $N = n_u + n_d$. Thus at leading order,

$$\chi_{20} = \left(\frac{T}{V}\right)\frac{Z_{20}}{Z} \qquad \chi_{11} = \left(\frac{T}{V}\right)\frac{Z_{11}}{Z} \tag{5}$$

Here $Z_{20} = Z[\langle \mathcal{O}_2 + \mathcal{O}_{11} \rangle]$, $Z_{11} = Z[\langle \mathcal{O}_{11} \rangle]$, $\mathcal{O}_1 = \mathrm{Tr}\ M^{-1}M'$,
$\mathcal{O}_2 = \mathcal{O}_1' = \mathrm{Tr}\ M^{-1}M'' - \mathrm{Tr}\ M^{-1}M'M^{-1}M'$, and
$\mathcal{O}_{11} = \mathcal{O}_1 \cdot \mathcal{O}_1 = (\mathrm{Tr}\ M^{-1}M')^2$.

Higher order NLS are more involved since higher derivatives of $\mathcal{O}$ with more quark propagators come into play; systematic evaluation procedure helpful to optimize the number of M-inversions.

At the next, 4^{th}, order we have

$$\begin{aligned} \chi_{40} &= \left(\frac{T}{V}\right)\left[\frac{Z_{40}}{Z} - 3\left(\frac{Z_{20}}{Z}\right)^2\right], \\ \chi_{31} &= \left(\frac{T}{V}\right)\left[\frac{Z_{31}}{Z} - 3\left(\frac{Z_{20}}{Z}\right)\left(\frac{Z_{11}}{Z}\right)\right], \\ \chi_{22} &= \left(\frac{T}{V}\right)\left[\frac{Z_{22}}{Z} - \left(\frac{Z_{20}}{Z}\right)^2 - 2\left(\frac{Z_{11}}{Z}\right)^2\right] \,, \end{aligned} \tag{6}$$

Higher order NLS are more involved since higher derivatives of $\mathcal{O}$ with more quark propagators come into play; systematic evaluation procedure helpful to optimize the number of M-inversions.

At the next, 4^{th}, order we have

$$\chi_{40} = \left(\frac{T}{V}\right)\left[\frac{Z_{40}}{Z} - 3\left(\frac{Z_{20}}{Z}\right)^2\right],$$

$$\chi_{31} = \left(\frac{T}{V}\right)\left[\frac{Z_{31}}{Z} - 3\left(\frac{Z_{20}}{Z}\right)\left(\frac{Z_{11}}{Z}\right)\right],$$

$$\chi_{22} = \left(\frac{T}{V}\right)\left[\frac{Z_{22}}{Z} - \left(\frac{Z_{20}}{Z}\right)^2 - 2\left(\frac{Z_{11}}{Z}\right)^2\right], \qquad (6)$$

with

$$
\begin{aligned}
Z_{40} &= Z\left\langle \mathcal{O}_{1111} + 6\mathcal{O}_{112} + 4\mathcal{O}_{13} + 3\mathcal{O}_{22} + \mathcal{O}_{4} \right\rangle, \\
Z_{31} &= Z\left\langle \mathcal{O}_{1111} + 3\mathcal{O}_{112} + \mathcal{O}_{13} \right\rangle, \\
Z_{22} &= Z\left\langle \mathcal{O}_{1111} + 2\mathcal{O}_{112} + \mathcal{O}_{22} \right\rangle.
\end{aligned} \tag{7}
$$

The 8th order, involves operators up to $\mathcal{O}_8$ which in turn have terms up to 8 quark propagators. In fact, the entire evaluation of the χ_{80} needs 20 inversions of Dirac matrix.

with

$$
\begin{aligned}
Z_{40} &= Z\left\langle \mathcal{O}_{1111} + 6\mathcal{O}_{112} + 4\mathcal{O}_{13} + 3\mathcal{O}_{22} + \mathcal{O}_{4} \right\rangle, \\
Z_{31} &= Z\left\langle \mathcal{O}_{1111} + 3\mathcal{O}_{112} + \mathcal{O}_{13} \right\rangle, \\
Z_{22} &= Z\left\langle \mathcal{O}_{1111} + 2\mathcal{O}_{112} + \mathcal{O}_{22} \right\rangle.
\end{aligned}
\tag{7}
$$

The 8th order, involves operators up to $\mathcal{O}_8$ which in turn have terms up to 8 quark propagators. In fact, the entire evaluation of the χ_{80} needs 20 inversions of Dirac matrix.

- Problem of finding the minimum number inversions for a given order — Akin to Steiner Problem in Computer Science $\rightsquigarrow$ our algorithm

- The traces are estimated by a stochastic method: $\mathrm{Tr}\ A = \sum_{i=1}^{N_v} R_i^\dagger A R_i / 2N_v$, and $(\mathrm{Tr}\ A)^2 = 2\sum_{i>j=1}^{L} (\mathrm{Tr}\ A)_i (\mathrm{Tr}\ A)_j / L(L-1)$, where R_i is a complex vector from an Gaussian ensemble of N_v which is further subdivided in L independent sets.

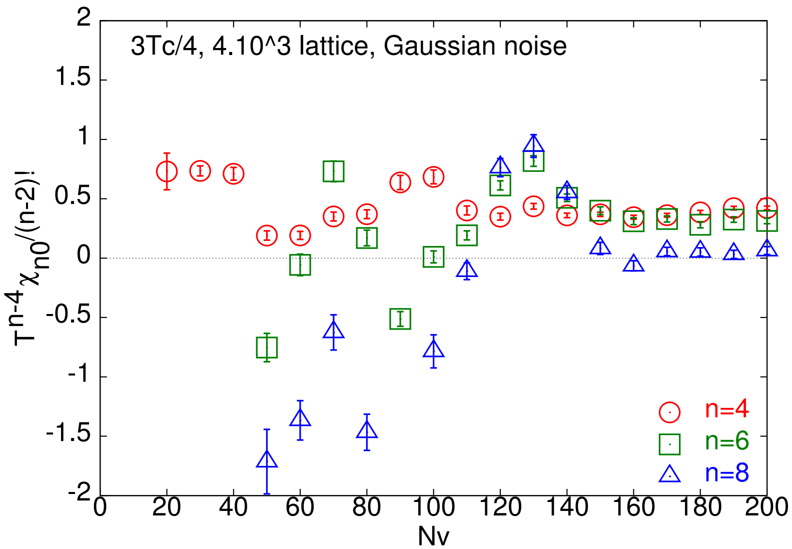

Higher NLS need larger N_v : Up to 500 used as N_s increased to 24.

- Problem of finding the minimum number inversions for a given order — Akin to Steiner Problem in Computer Science $\rightsquigarrow$ our algorithm

- The traces are estimated by a stochastic method: $\mathrm{Tr}\ A = \sum_{i=1}^{N_v} R_i^\dagger A R_i / 2N_v$, and $(\mathrm{Tr}\ A)^2 = 2 \sum_{i>j=1}^{L} (\mathrm{Tr}\ A)_i (\mathrm{Tr}\ A)_j / L(L-1)$, where R_i is a complex vector from an Gaussian ensemble of N_v which is further subdivided in L independent sets.

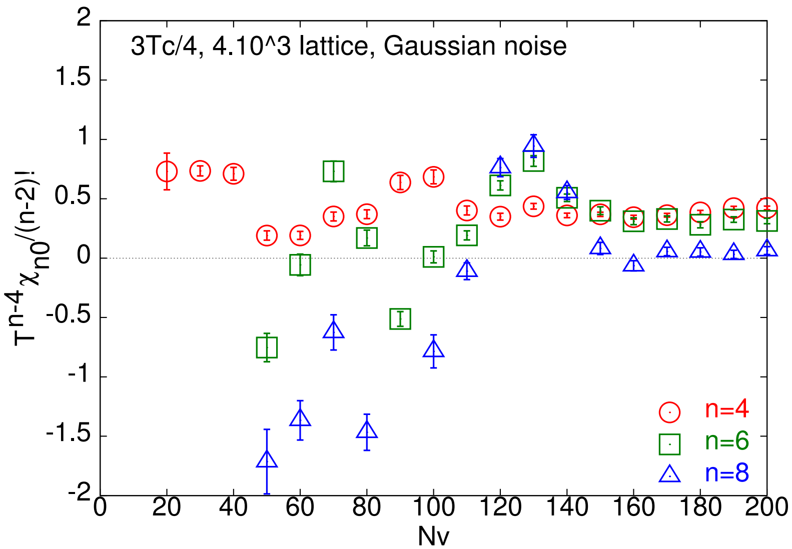

Higher NLS need larger N_v : Up to 500 used as N_s increased to 24.

- Problem of finding the minimum number inversions for a given order — Akin to Steiner Problem in Computer Science $\rightsquigarrow$ our algorithm

- The traces are estimated by a stochastic method: $\mathrm{Tr}\ A = \sum_{i=1}^{N_v} R_i^\dagger A R_i / 2N_v$, and $(\mathrm{Tr}\ A)^2 = 2 \sum_{i>j=1}^{L} (\mathrm{Tr}\ A)_i (\mathrm{Tr}\ A)_j / L(L-1)$, where R_i is a complex vector from an Gaussian ensemble of N_v which is further subdivided in L independent sets.

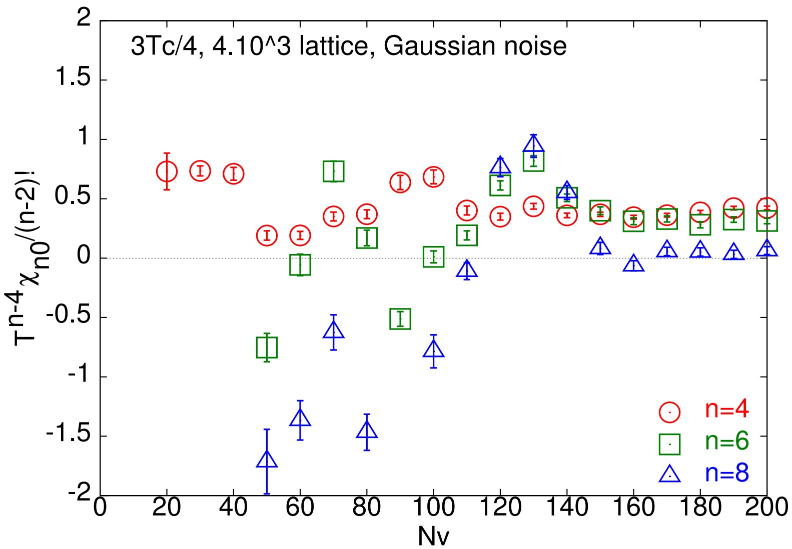

Higher NLS need larger N_v : Up to 500 used as N_s increased to 24.

Our Simulations & Results

- Lattice used : 4 $\times N_s^3$, $N_s =$ 8, 10, 12, 16, 24
- Staggered fermions with $N_f = 2$ of $m/T_c = 0.1$; R-algorithm with traj. length of 1 MD time on $N_s = 8$, scaled $\propto N_s$ on larger ones.
- $m_\rho/T_c = 5.4 \pm 0.2$ and $m_\pi/m_\rho = 0.31 \pm 0.01$ (MILC)

Our Simulations & Results

- Lattice used : 4 $\times N_s^3$, N_s = 8, 10, 12, 16, 24
- Staggered fermions with $N_f = 2$ of $m/T_c = 0.1$; R-algorithm with traj. length of 1 MD time on $N_s = 8$, scaled $\propto N_s$ on larger ones.
- $m_\rho/T_c = 5.4 \pm 0.2$ and $m_\pi/m_\rho = 0.31 \pm 0.01$ (MILC)
- Simulations made at T/T_c = 0.75(2), 0.80(2), 0.85(1), 0.90(1), 0.95(1), 0.975(10), 1.00(1), 1.05(1), 1.25(1), 1.65(6) and 2.15(10)
- Typical stat. 50-100 in max autocorrelation units.

Quark Number Susceptibility

- Proposed as a signal of light quarks in QGP (McLerran '87).

Quark Number Susceptibility

- Proposed as a signal of light quarks in QGP (McLerran '87).
- Early results near T_c displayed order-parameter like behaviour in full QCD (Gottlieb et al. '87)
- And quenched QCD (Gavai et al. '89).

Quark Number Susceptibility

- Proposed as a signal of light quarks in QGP (McLerran '87).
- Early results near T_c displayed order-parameter like behaviour in full QCD (Gottlieb et al. '87)
- And quenched QCD (Gavai et al. '89).

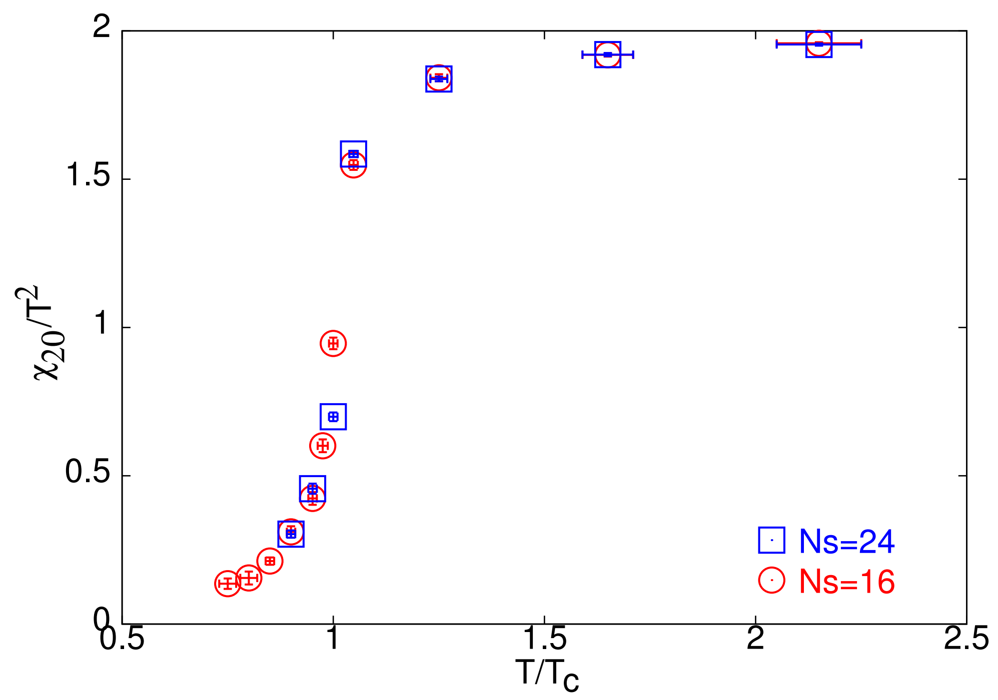

Quark Number Susceptibility

- Proposed as a signal of light quarks in QGP (McLerran '87).
- Early results near T_c displayed order-parameter like behaviour in full QCD (Gottlieb et al. '87)
- And quenched QCD (Gavai et al. '89).

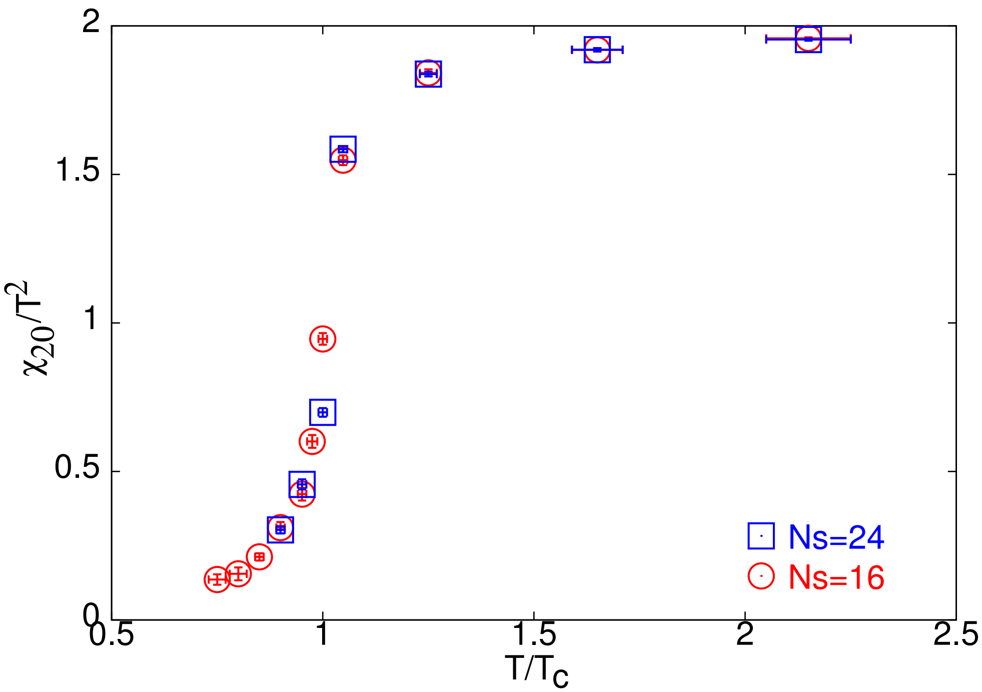

♠ Fluctuations, Wroblewski Parameter ....
♠ Comparison with weak coupling.

♠ Interesting to note that χ_{40} shows the same volume dependence at T_c as χ_L which in turn comes from the $\langle \mathcal{O}_{22} \rangle_c$.

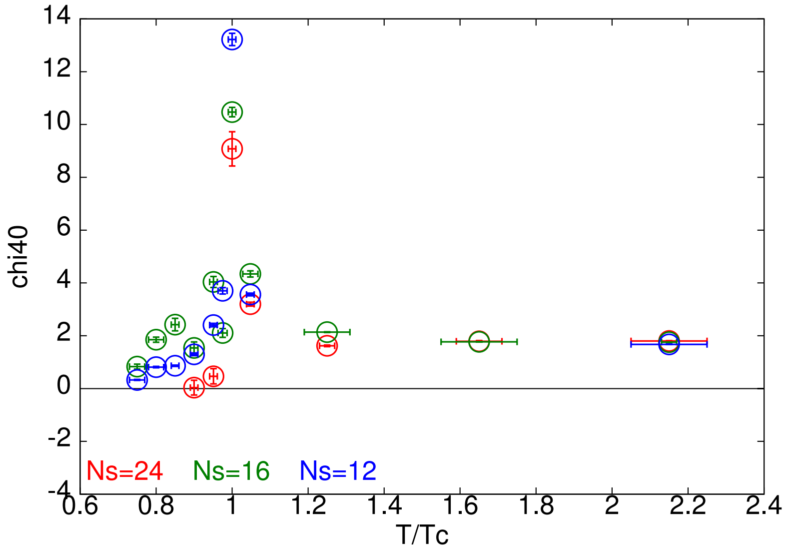

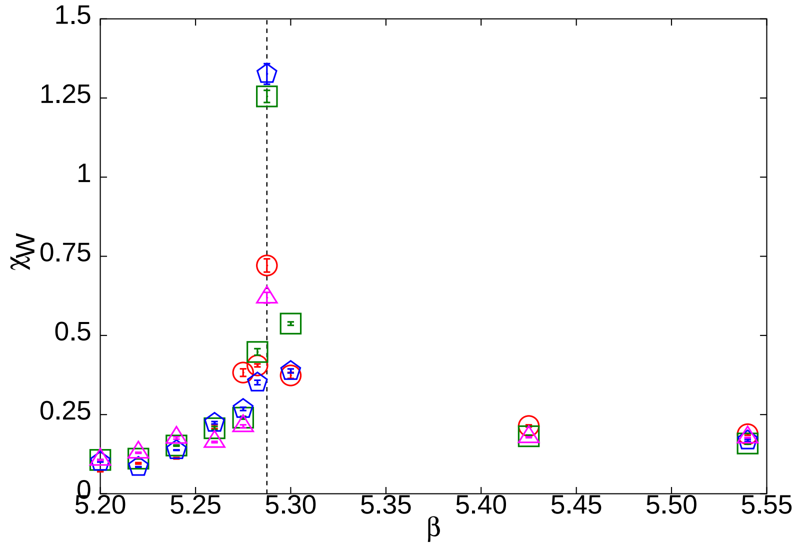

♠ Interesting to note that χ_{40} shows the same volume dependence at T_c as χ_L which in turn comes from the $\langle \mathcal{O}_{22} \rangle_c$.

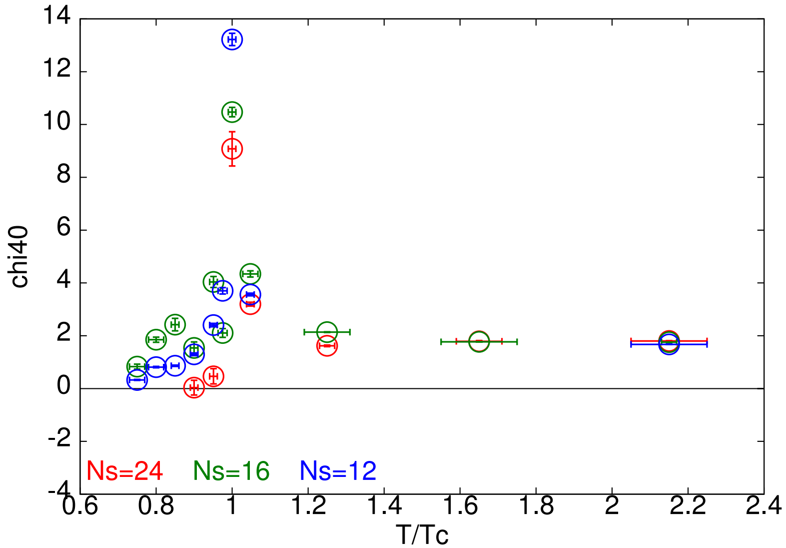

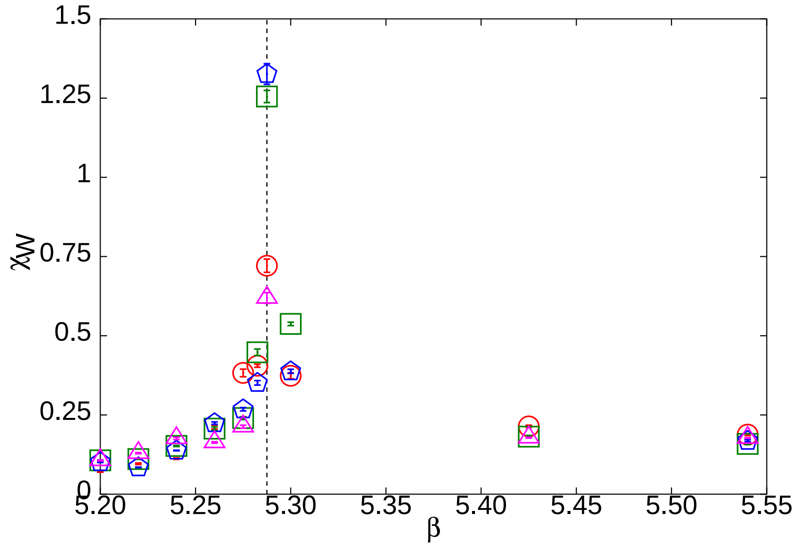

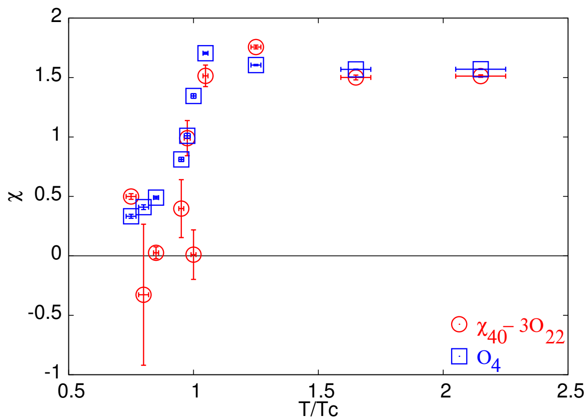

♠ Interesting to note that χ_{40} shows the same volume dependence at T_c as χ_L which in turn comes from the $\langle \mathcal{O}_{22} \rangle_c$.

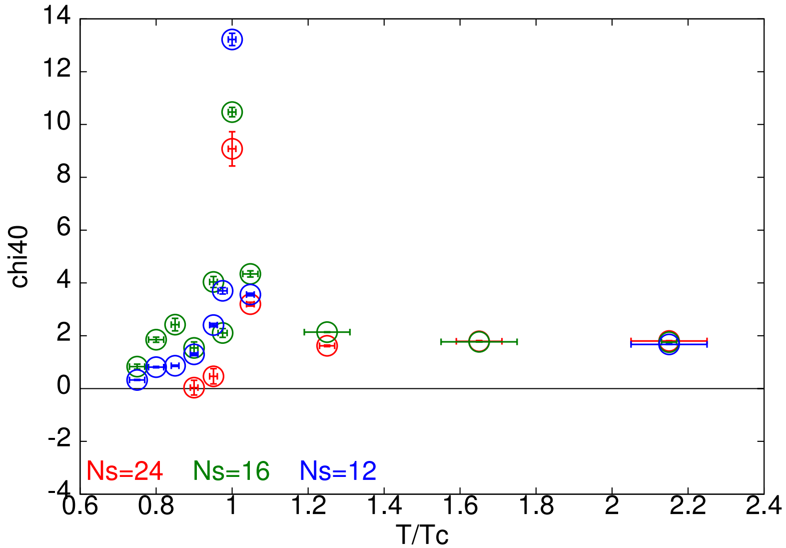

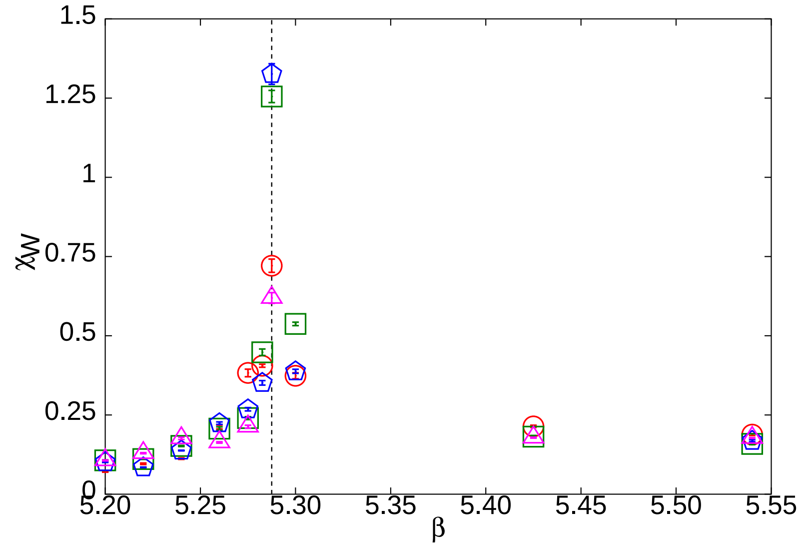

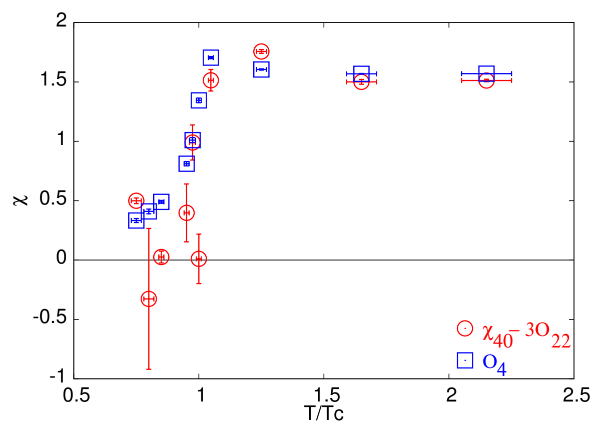

♠ Similar behaviour for higher order terms as well: $\langle \mathcal{O}_{222} \rangle_c$, $\langle \mathcal{O}_{2222} \rangle_c$.....

More Details

Measure of the seriousness of sign problem : Ratio χ_{11}/χ_{20}

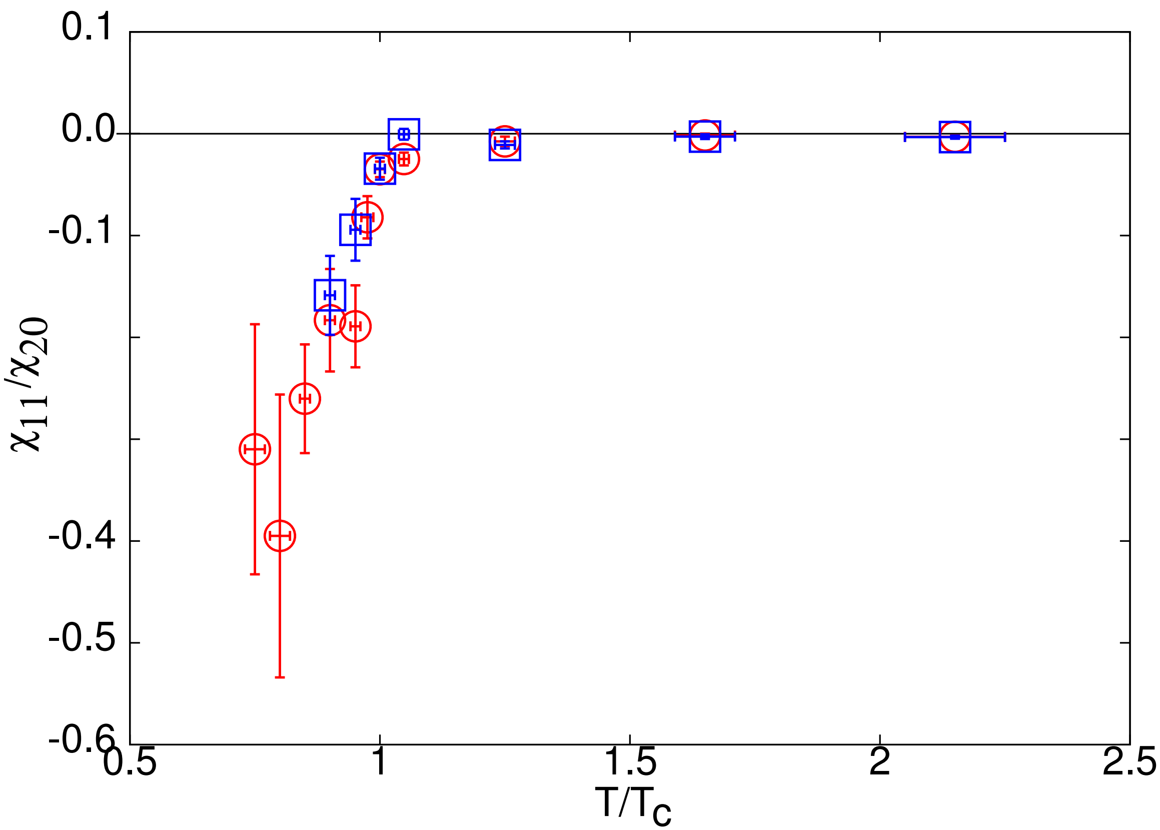

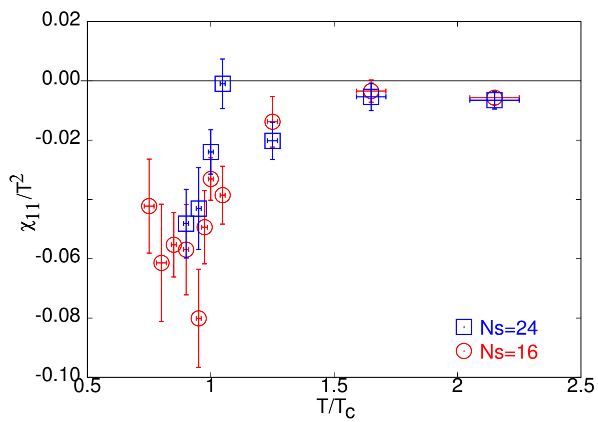

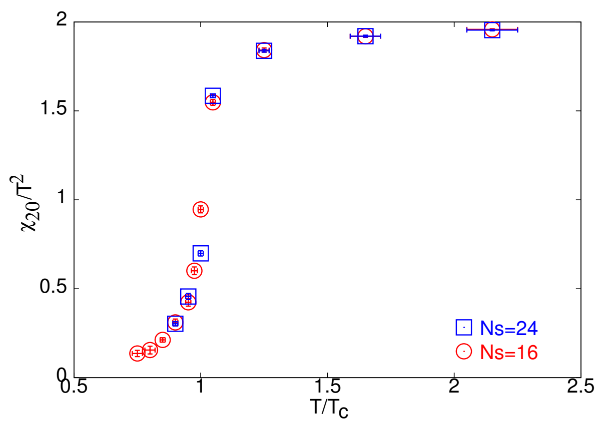

Volume Dependence

♠ Each coefficient in the Taylor expansion must be volume independent.

♠ Nontrivial check on lattice computations since there are diverging terms which have to cancel.

Volume Dependence

♠ Each coefficient in the Taylor expansion must be volume independent.

♠ Nontrivial check on lattice computations since there are diverging terms which have to cancel.

♠ We had earlier suggested to obtain more pairs of diverging terms by taking larger N_f.

♠ E.g. $T/V \langle \mathcal{O}_{22} \rangle_c$ should be finite as it is a combination of Taylor Coeffs.

Volume Dependence

♠ Each coefficient in the Taylor expansion must be volume independent.

♠ Nontrivial check on lattice computations since there are diverging terms which have to cancel.

♠ We had earlier suggested to obtain more pairs of diverging terms by taking larger N_f.

♠ E.g. $T/V \langle \mathcal{O}_{22} \rangle_c$ should be finite as it is a combination of Taylor Coeffs.

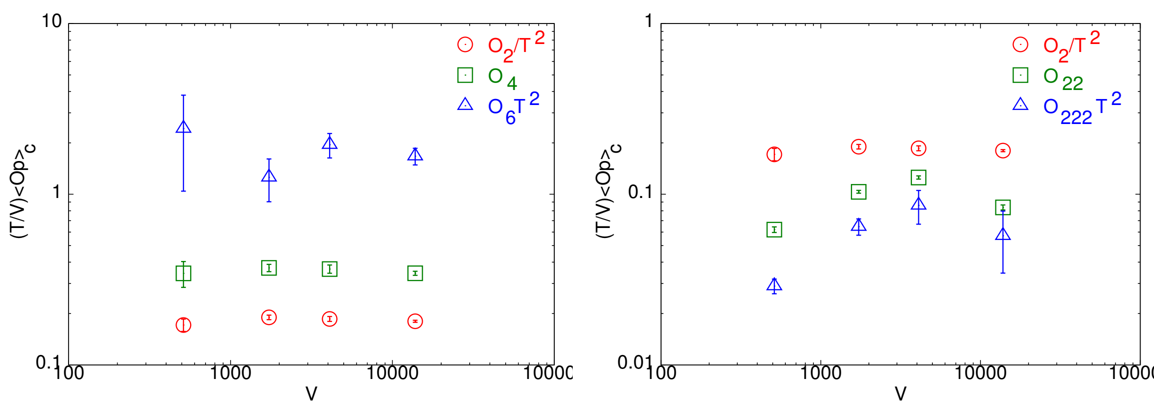

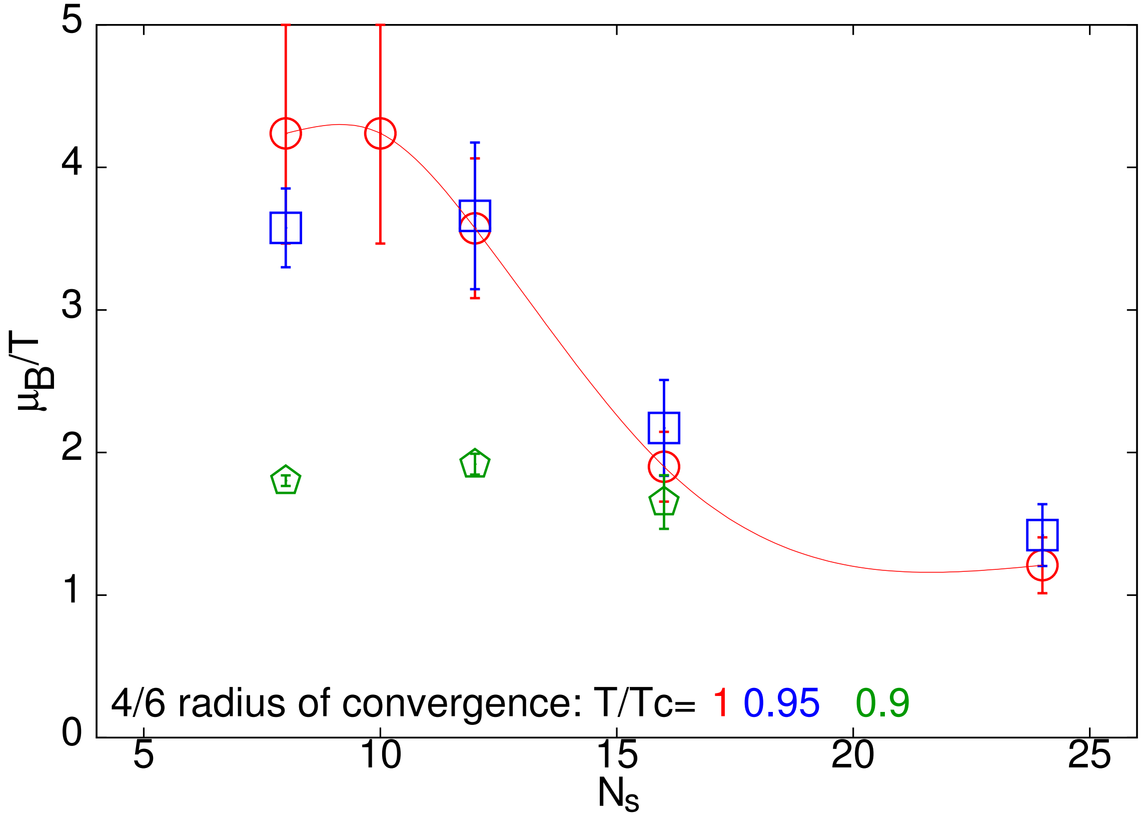

5
4
3
2
1
0
μ_B/T
5
10
15
20
25
N_s
4/6 radius of convergence: T/Tc= 1 0.95 0.9

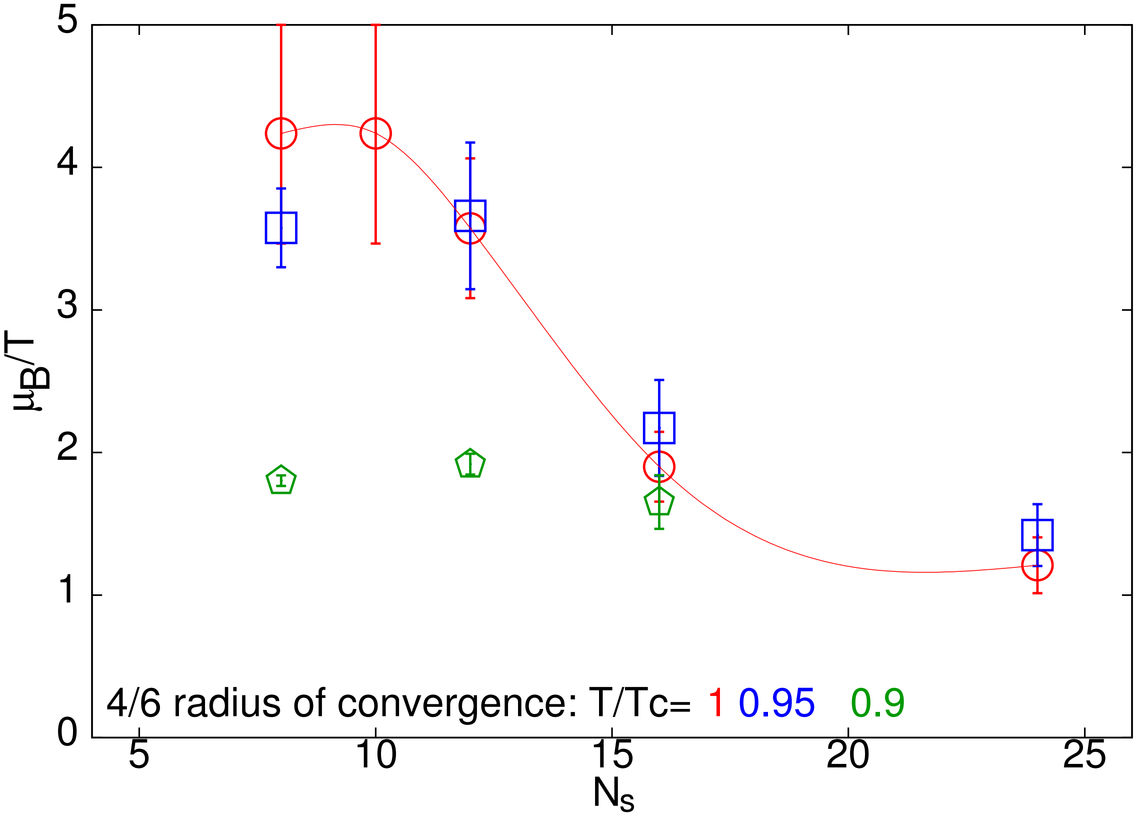

- Strong finite size effects for small N_s. A strong change around $N_s \sim 14$ or $N_s m_\pi \sim 6$. (Compatible with arguments of Smilga & Leutwyler and also seen for i) hadron masses by Gupta & Ray and ii) DIS structure functions by ZeRo Collaboration, Gaugnelli et al. PLB '04)

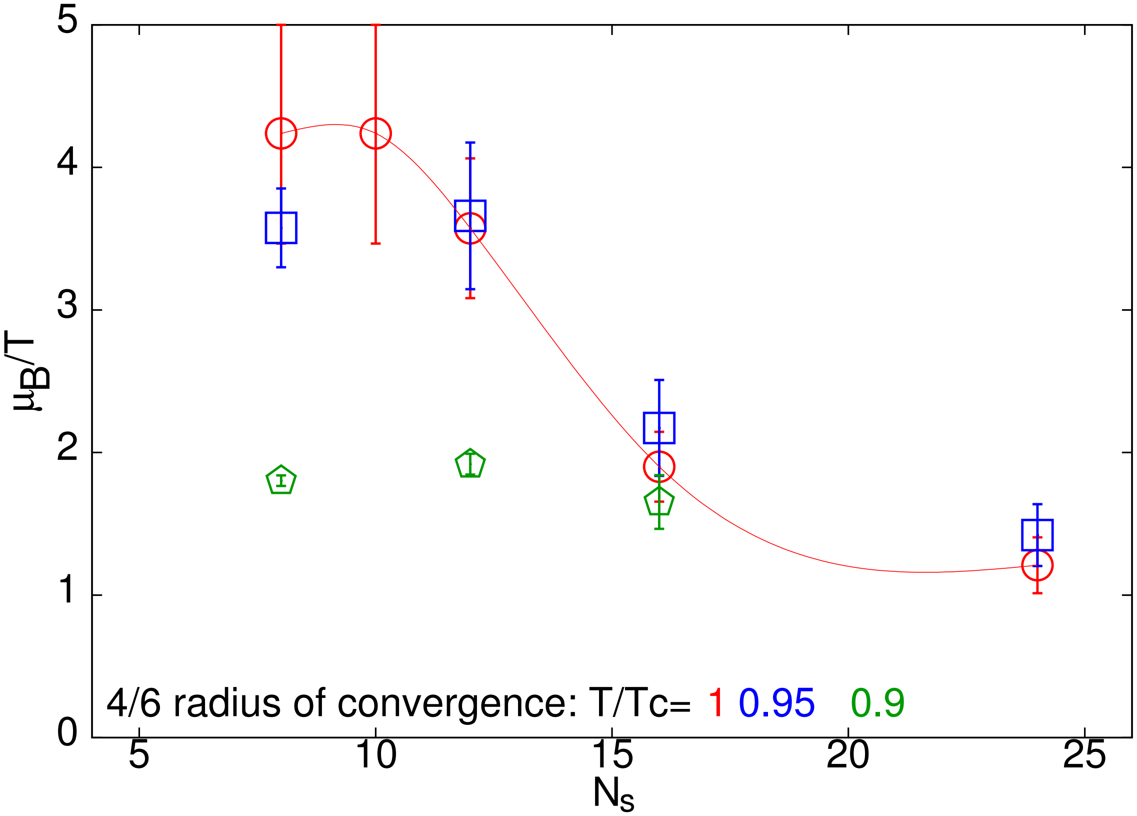

- Strong finite size effects for small N_s. A strong change around $N_s \sim 14$ or $N_s m_\pi \sim 6$. (Compatible with arguments of Smilga & Leutwyler and also seen for i) hadron masses by Gupta & Ray and ii) DIS structure functions by ZeRo Collaboration, Gaugnelli et al. PLB '04)

- Bielefeld results for $N_s m_\pi \sim 15$ but large $m_\pi/m_\rho \sim 0.7$.

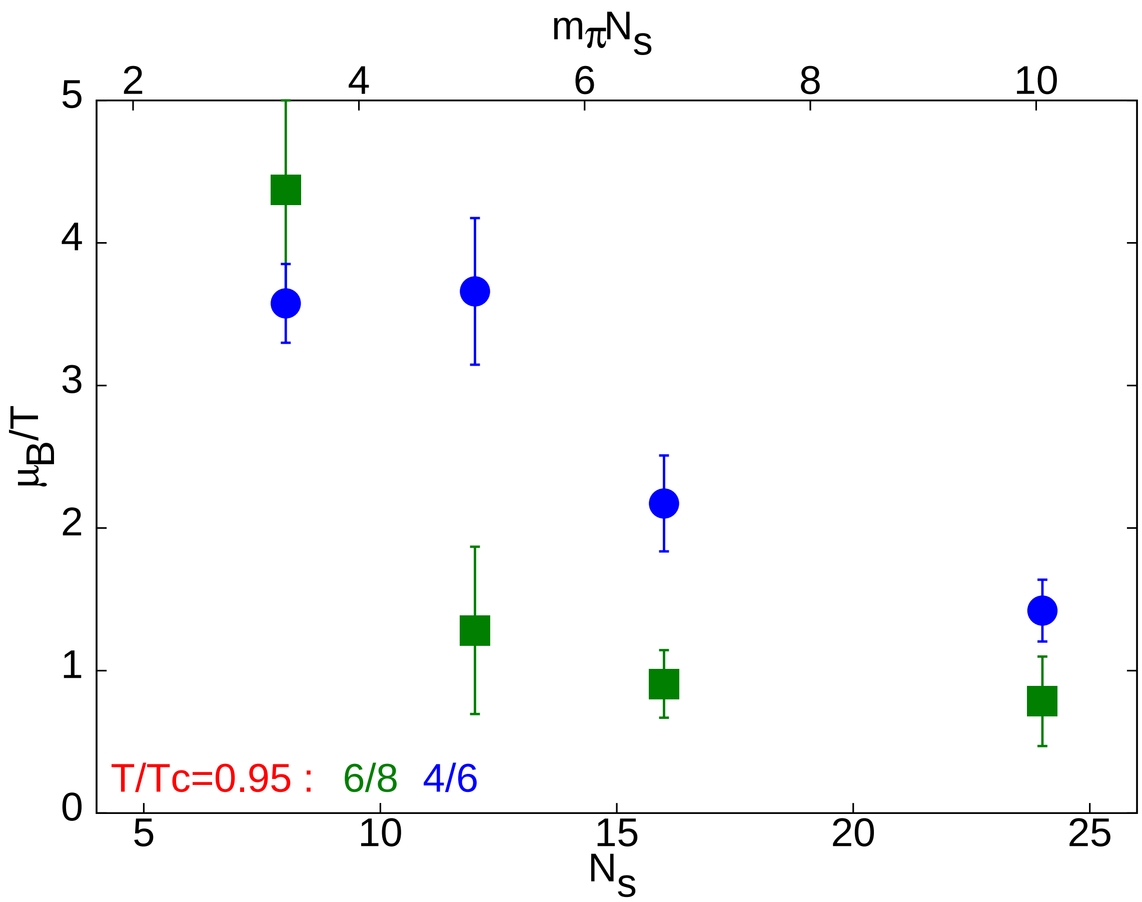

$m_\pi N_S$
2
4
6
8
10
5
4
3
2
1
0
μ_B/T
T/Tc=0.95 :
6/8
4/6
5
10
15
20
25
N_S

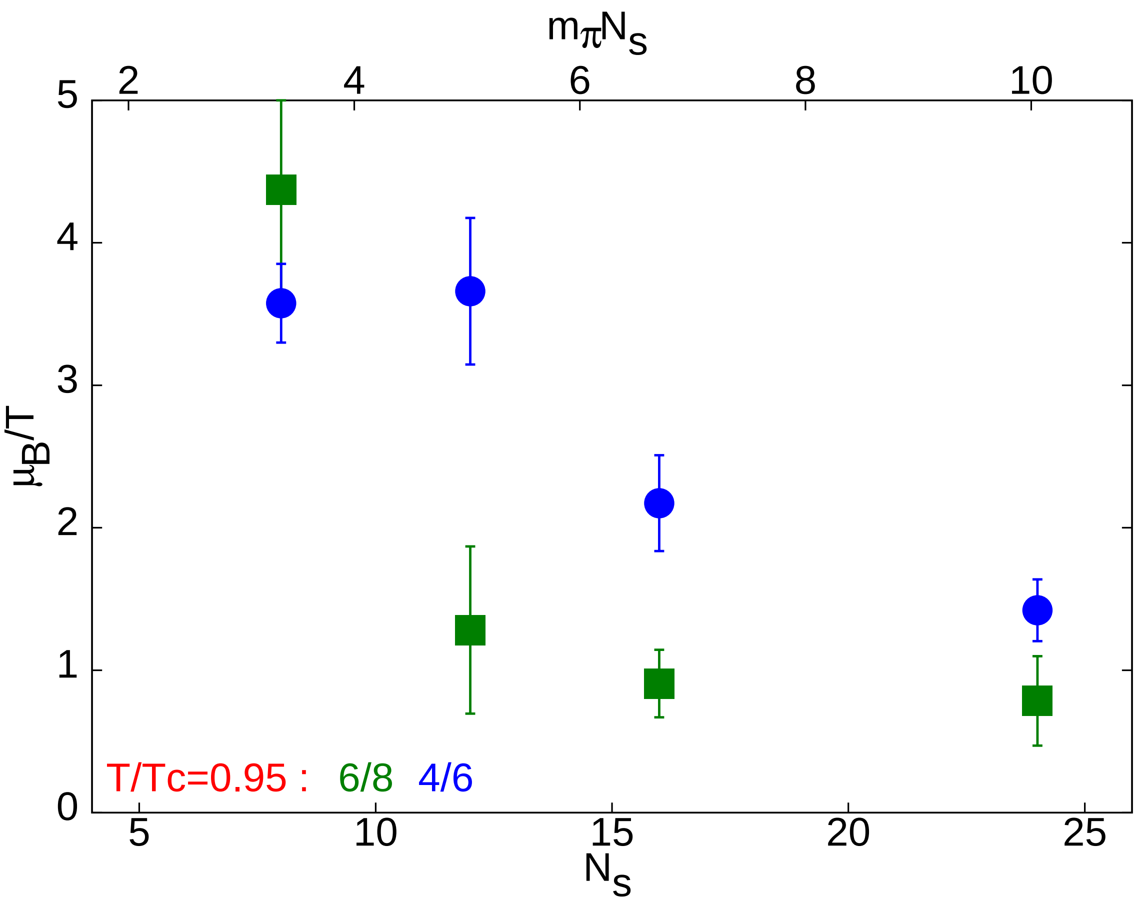

- Our estimate consistent with Fodor & Katz (2002) [$m_\pi/m_\rho = 0.31$ and $N_s m_\pi \sim$ 3-4].

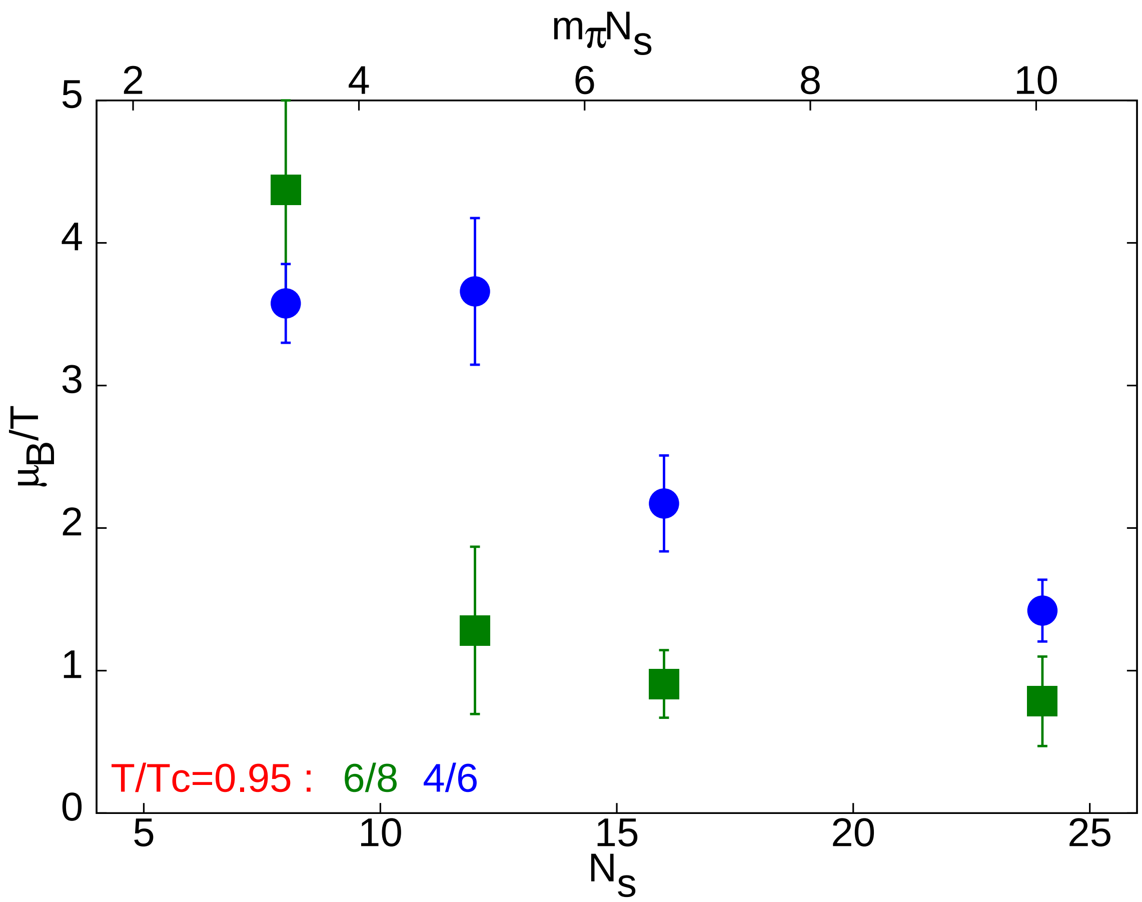

- Our estimate consistent with Fodor & Katz (2002) [$m_\pi/m_\rho = 0.31$ and $N_s m_\pi \sim$ 3-4].
- Critical point shifted to smaller $\mu_B/T \sim 1 - 2$.

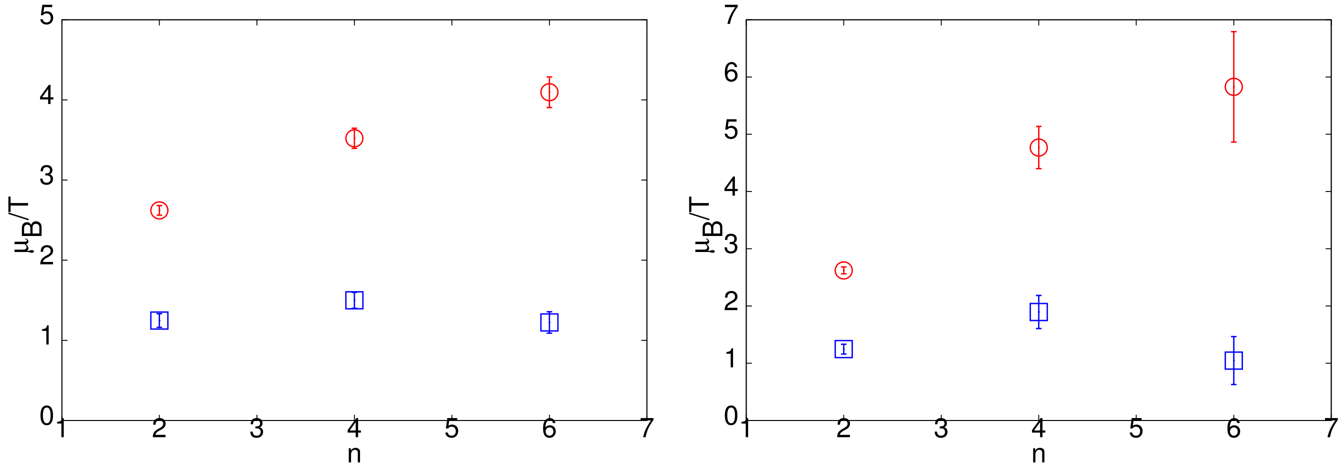

μB/T
n
μB/T
n

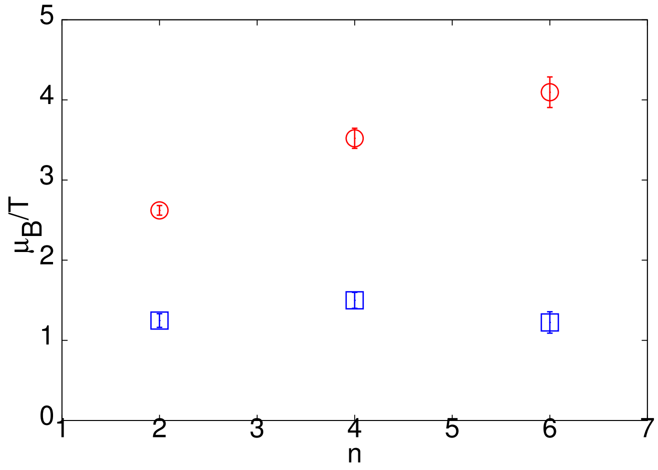

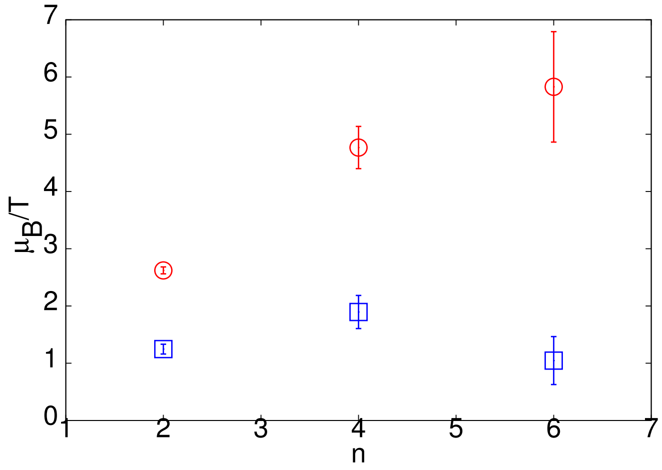

♠ Radii of convergence as a function of the order of expansion at $T = 0.95T_c$ on $N_s = 8$ (circles) and 24 (boxes).

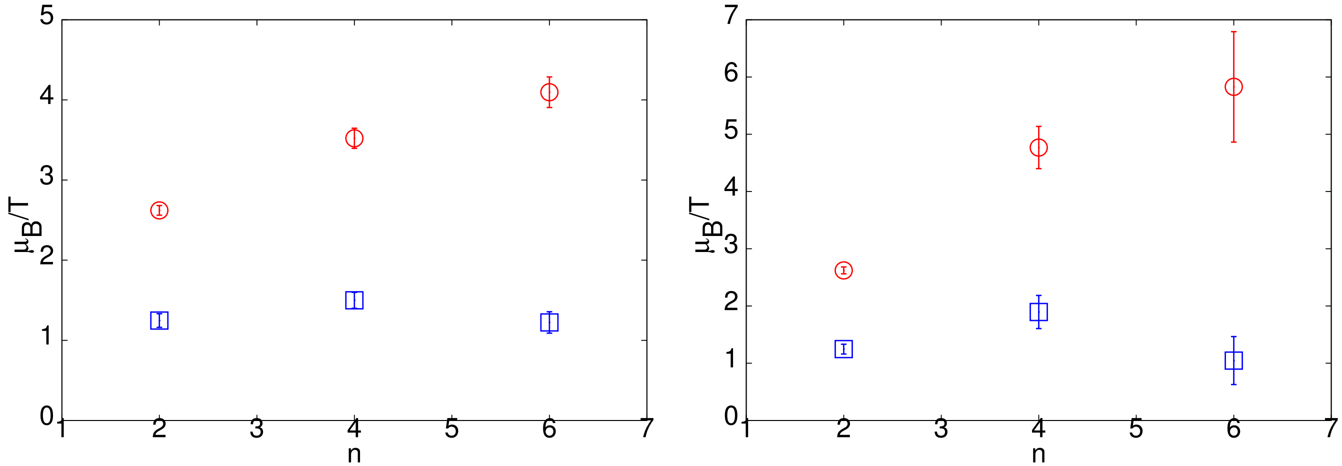

♠ Radii of convergence as a function of the order of expansion at $T = 0.95T_c$ on $N_s = 8$ (circles) and 24 (boxes).

♠ Left panel for ρ_n and right one for r_n.
Extrapolation in $n \rightsquigarrow \mu^E/T^E = 1.1 \pm 0.2$ at $T^E = 0.95T_c$.

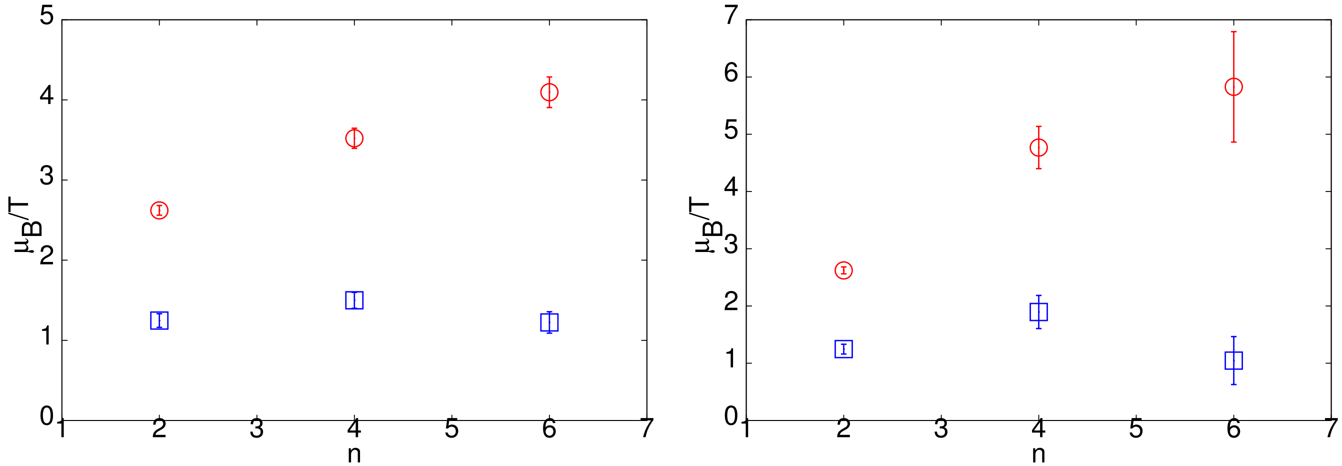

♠ Radii of convergence as a function of the order of expansion at $T = 0.95T_c$ on $N_s = 8$ (circles) and 24 (boxes).

♠ Left panel for ρ_n and right one for r_n.
Extrapolation in $n \rightsquigarrow \mu^E/T^E = 1.1 \pm 0.2$ at $T^E = 0.95T_c$.

♠ Finite volume shift consistent with Ising Universality class.

Summary

- Phase diagram in $T - \mu$ on $N_t = 4$ has begun to emerge: Different methods, $\rightsquigarrow$ similar qualitative picture.

Summary

- Phase diagram in $T - \mu$ on $N_t = 4$ has begun to emerge: Different methods, $\rightsquigarrow$ similar qualitative picture.

- Volume independence provides check on the computation from cancellations in connected terms

Summary

- Phase diagram in $T-\mu$ on $N_t = 4$ has begun to emerge: Different methods, $\rightsquigarrow$ similar qualitative picture.
- Volume independence provides check on the computation from cancellations in connected terms
- Our results on volume dependence suggest $N_s m_\pi > 6$ in thermodynamic volume limit. μ_B/T of critical end point shows a strong drop at that volume.

Summary

- Phase diagram in $T - \mu$ on $N_t = 4$ has begun to emerge: Different methods, $\rightsquigarrow$ similar qualitative picture.
- Volume independence provides check on the computation from cancellations in connected terms
- Our results on volume dependence suggest $N_s m_\pi > 6$ in thermodynamic volume limit. μ_B/T of critical end point shows a strong drop at that volume.
- $\mu_B/T \sim 1 - 2$ is indicated for the critical point. Larger N_t would be interesting.

QCD Phase Diagram : 2005

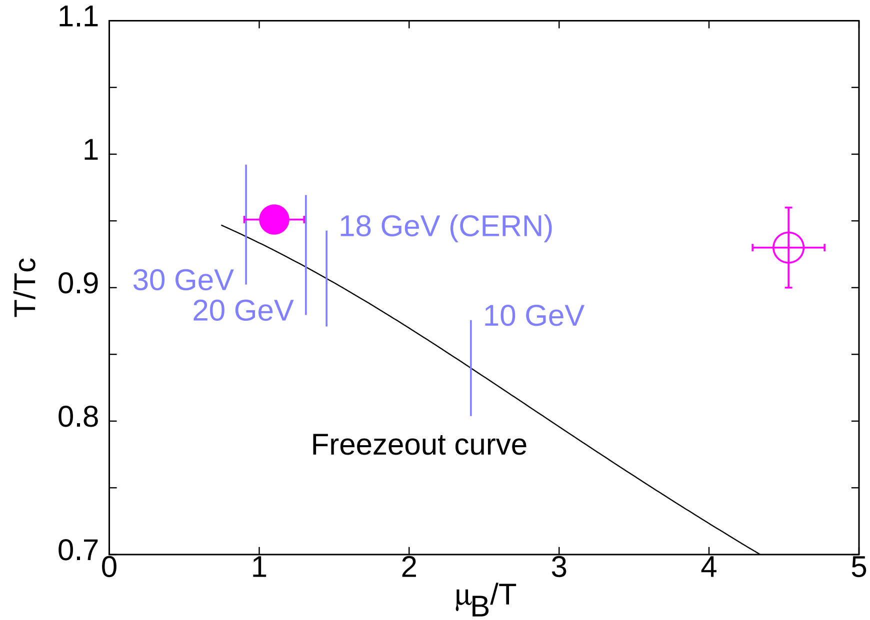

QCD Phase Diagram : 2005

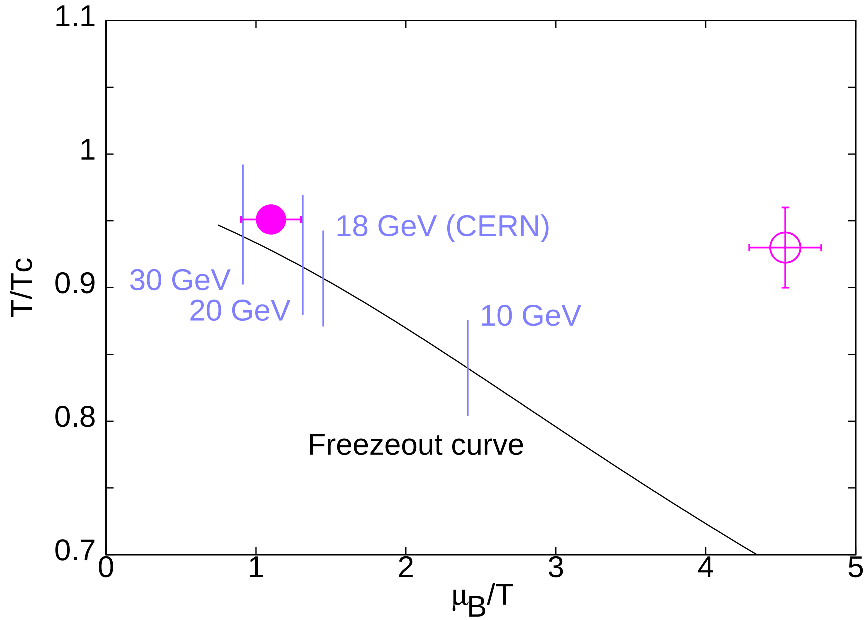

- Our result shown by solid point; Fodor-Katz '02 point (same quark mass) also shown. Freezout Curves from Cleymans using T_c in our case.

QCD Phase Diagram : 2005

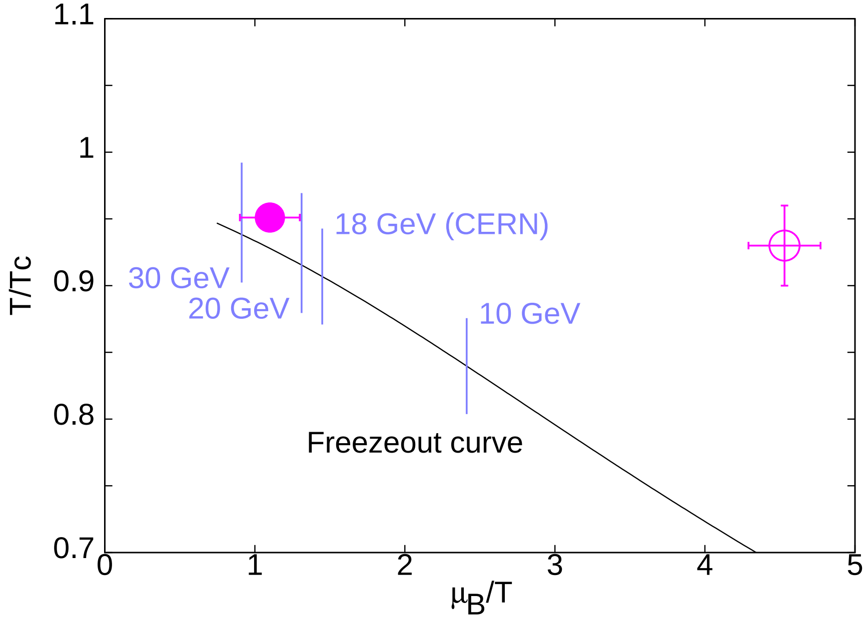

- Our result shown by solid point; Fodor-Katz '02 point (same quark mass) also shown. Freezout Curves from Cleymans using T_c in our case.

- References : RVG and Sourendu Gupta, PRD, 71, 114014 (2005) and PRD 72, 054006 (2005).

m_ρ/T_c	m_π/m_ρ	m_N/m_ρ	$N_s m_\pi$	flavours	T^E/T_c	μ_B^E/T^E
5.372 (5)	0.185 (2)	—	1.9–3.0	2+1	0.99 (2)	2.2 (2)
5.12 (8)	0.307 (6)	—	3.1–3.9	2+1	0.93 (3)	4.5 (2)
5.4 (2)	0.31 (1)	1.8 (2)	3.3–10.0	2	0.95 (2)	1.1 (2)
5.4 (2)	0.31 (1)	1.8 (2)	3.3	2	—	—
5.5 (1)	0.70 (1)	—	15.4	2	—	—

Table 1: Summary of critical end point estimates— the lattice spacing is $a = 1/4T$. N_s is the spatial size of the lattice and $N_s m_\pi$ is the size in units of the pion Compton wavelength, evaluated for $T = \mu = 0$. The ratio m_π/m_K sets the scale of the strange quark mass.

Results are sequentially from Fodor-Katz '04, Fodor-Katz '02, Gavai-Gupta, de Forcrand- Philipsen and Bielefeld-Swansea.